Article

Effect of Synthetic Polypeptide–*Bio*-Surfactant Composition on the Formation and Stability of Foams

Dominik Kosior *[iD], Agata Wiertel-Pochopien [iD], Maria Morga, Łukasz Witkowski [iD] and Jan Zawala [iD]

Jerzy Haber Institute of Catalysis and Surface Chemistry, Polish Academy of Sciences, Niezapominajek 8, 30-239 Krakow, Poland; agata.wiertel-pochopien@ikifp.edu.pl (A.W.-P.); maria.morga@ikifp.edu.pl (M.M.); lukasz.witkowski@ikifp.edu.pl (Ł.W.); jan.zawala@ikifp.edu.pl (J.Z.)
* Correspondence: dominik.kosior@ikifp.edu.pl

Abstract: In recent decades, numerous studies have focused on finding environmentally friendly substitutes for commonly used petrochemical-based compounds. This paper explores the potential use of poly-L-lysine/rhamnolipids and poly-L-glutamic acid/ethyl lauroyl arginate mixtures, for foam formation and stabilization. Two complementary methods were employed to investigate the synergistic and antagonistic effects of these mixed polyelectrolyte/surfactant systems: (1) the thinning and rupture of thin foam films formed under dynamic conditions were monitored using a dynamic fluid-film interferometer (DFI), and (2) foamability tests were conducted using a standard dynamic foam analyzer (DFA). The results demonstrated that adding polyelectrolyte to an oppositely charged surfactant primarily induces a synergistic effect, enhancing foaming properties and extending foam lifetime. Furthermore, interferometric methods confirmed improved stability and slower drainage of thin foam films in systems containing synthetic polypeptides.

Keywords: polyelectrolyte/surfactants systems; foam stability; thin foam film; bio-surfactants; synthetic polypeptides; rhamnolipids; ethyl lauroyl arginate; poly-L-lysine; poly-L-glutamic acid

1. Introduction

Foams represent one of the largest groups of dispersed systems and are widely utilized in industrial, technological, and everyday applications. Examples of the significant demand for foam products include mineral processing [1,2], the food industry [3], firefighting [4], cleaning agents [5], and cosmetic and pharmaceutical applications [6]. Recently, the search for foams capable of responding to external stimuli such as temperature, light, or electricity has been of growing interest [7,8]. Mixed polyelectrolyte/surfactant (PE/S) systems for the stabilization of foams and emulsions have been investigated and applied in modern technologies [9–11]. So far, PE/S systems have found applications in detergency, drug delivery, rheological modifiers, and cosmetics [12,13]. On the other hand, polymers have also been adapted for use in mineral processing technologies such as froth flotation [14,15] and flocculation [16] and thus might present an interesting alternative to nanoparticle/surfactant compositions [17,18]. Therefore, it is of great importance to explore polyelectrolyte–surfactant interactions and their effects on process efficiency in these applications.

The stability of foams is primarily governed by the stability of the microscopic and mesoscopic thin liquid films between the compartments (air bubbles). The interfacial behavior of long alkyl chain polyelectrolytes is strongly influenced by hydrophobic interactions, while the complex formation with short-chain surfactants is dominated by electrostatic interactions. In the case of quasi-static single standoff foam films, the general observation is that the stabilization via oppositely charged PE/S mixtures leads to stable common black films (CBFs), while other systems (same charge system, or non-ionic/charged compounds system) usually form thinner and less stable Newton black films (NBFs) [19]. Beyond these

general rules, the preparation of PE/S systems with desirable features depends on several physicochemical properties, including the charge and hydrophobicity of the compounds used, PE chain length and conformation, PE/S ratio, type of surfactant's headgroup, as well as the bulk's pH and ionic strength [20–24].

Unfortunately, despite their effectiveness in formulation processes, most commonly used polyelectrolytes and surfactants are petrochemical-based compounds that decompose slowly in the natural environment, contributing to water pollution, eutrophication of water bodies, and accumulation in living organisms [25,26]. Those effects are especially pronounced in mineral industry processes where large numbers of chemical compounds are used, such as in froth flotation [27,28], bitumen extraction [29], and enhanced oil recovery [30]. To counteract these undesirable effects, it is of great importance to search for biodegradable, environmentally friendly compounds with low toxicity for both humans and the environment, especially in terms of mass production and overuse of surfactant systems. This problem can be partially addressed by replacing the standard formulation with bio-surfactants, which offer a more environmentally friendly alternative [31–33]. Bio-surfactants have the potential to reduce the environmental impact of conventional surfactants while maintaining similar or improved performance in various industrial applications, such as mineral flotation [34–36], the petroleum industry [37,38], and water treatment [39,40]. In general, bio-surfactants have shown their efficacy in these applications, suggesting a promising shift toward more environmentally friendly practices.

The main objective of the presented study is to investigate the potential use of bio-polyelectrolytes and bio-surfactants in the stabilization of foam films formed under dynamic conditions. The choice of the PE/S system components was driven by their properties, such as biodegradability, biological activity (antiseptic properties), and biocompatibility. The physicochemical properties of the system and each component individually will play an important role in the formation and stabilization of thin liquid films.

Particular attention was paid to the potential use of bio-polyelectrolytes based on synthetic polyaminoacids: the polycation poly-L-lysine (PLL) and the polyanion poly-L-glutamic acid (PGA). Both macroions have attracted special interest due to their unique properties and their environmentally friendly, biocompatible behavior [41,42].

Regarding bio-surfactants, rhamnolipids (RH), and ethyl lauroyl arginate (LAE) were chosen. Rhamnolipids belong to the group of microbial glycolipids. They are defined as an anionic surfactants [43], but their charge is strongly dependent on the solution's pH [44,45]. They are considered 'green surfactants' due to their low toxicity, good biodegradability, and microbial origin. These properties make them an interesting replacement for standard surface-active compounds used in the industry [46,47]. Ethyl lauroyl arginate is an amino acid-based cationic surfactant [48] with strong antimicrobial activity [49]. It has been found that, when combined with cellulose nanocrystals, it forms stable and environmentally friendly foams [50,51], which makes it interesting in terms of PE/S systems.

Using a complementary approach—applying experimental techniques to study foam films under dynamic conditions—the synergistic and antagonistic effects of mixed poly-electrolyte/surfactant systems on foam film stability were examined.

2. Materials and Methods

2.1. Materials

Poly-L-lysine hydrobromide (PLL) of molecular weight 70–150 kg/mol and poly-L-glutamic acid sodium salt (PGA) of molecular weight 50–100 kg/mol were purchased from Sigma-Aldrich (Merck KGaA, Darmstadt, Germany). Stock suspensions of polyelectrolytes of concentration 1.0 g/dm^3 were prepared in Milli-Q water.

Rhamnolipid biosurfactant (RH) was purchased from AGAE Technologies LLC (Corvallis, OR, USA) as a mixture of different mono- and di-RA homologs. The exact composition of the RH mixture was studied by Legawiec et al. (2023) [45]. A stock solution of 1 g/dm^3 was prepared in Milli-Q water.

Ethyl lauroyl arginate (LAE) of molecular weight 421 g/mol was purchased from the United States Pharmacopeia Reference Standard (Frederick, MD, USA). A stock solution of 1.68 g/dm^3 (4×10^{-3} mol/dm^3) was prepared in pure water, stored in a fridge, and used within 3 days to avoid the influence of the surfactant hydrolysis products [52].

The ionic strength and the pH of solutions were adjusted using respective solutions of analytical grade NaCl (Merck KGaA, Darmstadt, Germany), NaOH, and HCl (Chempur, Piekary Slaskie, Poland). The pH of all measured solutions, unless otherwise mentioned, was in the range of 5.6–6.0.

All necessary solutions were obtained by dilution of the stock solutions. Milli-Q water (Millipore, Burlington, MA, USA) was used throughout the preparation of all solutions.

2.2. Methods

2.2.1. Physicochemical Characterization of Polyelectrolytes

The diffusion coefficients, D, of polyelectrolyte molecules were determined by the dynamic light scattering (DLS) using the Malvern Zetasizer Nano ZS apparatus (Malvern Panalytical, Malvern, UK). Knowing the diffusion coefficient, one can calculate the hydrodynamic diameter, d_H, of the molecules using the Stokes–Einstein relationship [53]:

$$d_H = \frac{kT}{3\pi\eta D} \tag{1}$$

where k is the Boltzmann constant, T is the absolute temperature, and η is the dynamic viscosity of the solution.

The electrophoretic mobility, μ_e, of polyelectrolyte molecules was measured by the laser Doppler velocimetry technique (LDV) using the same Malvern apparatus. The zeta potential, ζ, of the molecules was calculated using the Henry formula [53]:

$$\zeta = \frac{3\eta\mu_e}{2\varepsilon f(\kappa d_H)} \tag{2}$$

where ε is the electric permittivity of the electrolyte, and $f(\kappa d_H)$ is the Henry correction function.

2.2.2. Surface Tension Measurements

The surface tension, σ, measurements were performed using the bubble profile analysis tensiometer PAT-1 (Sinterface Technologies, Berlin, Germany). An air bubble was formed at the tip of a U-shaped steel capillary of 1 mm inner and 2 mm outer diameters in a closed cuvette (3.5 cm $\times$ 3.5 cm $\times$ 3.5 cm) filled with studied solution. To attain equilibrium, the emerging bubble was retained for 10,000–40,000 s.

The critical micelle concentrations (CMC) for both surfactants were determined by extrapolating the surface tension dependencies at low and high concentrations to the point of intersection.

2.2.3. Dynamic Foam Analysis

Foamability and foam stability of pure surfactants and their mixture with polyelectrolytes were measured using a Dynamic Foam Analyzer DFA100 (Kruss GmbH, Hamburg, Germany) [54]. The apparatus consisted of (i) a cylindrical glass column of 40 mm diameter and of 250 mm height and (ii) light scanners for simultaneous automatic measurement of foam and solution heights as a function of time. Before each measurement, the cylindrical column was carefully cleaned with 5% Mucasol (Schülke and Mayr GmbH, Norderstedt, Germany) solution and thoroughly rinsed with Milli-Q water. Next, the column was placed on the apparatus stand and filled with 50 cm^3 of the studied solution. The foam was produced by the air pumped at a flow rate of 0.5 dm^3/min for 20 s through the air disperser—pure cellulose filter paper with pore sizes 12–15 µm. Data (foam height) grabbed by PC were analyzed by Kruss Advance software. All measurements were repeated at least three times.

The data on foaminess and foam decay were gathered and used for the calculation of the Bikerman unit of foaminess [55] and the foam production [56]. The Bikerman unit of foaminess, Σ, is defined as [55]:

$$\Sigma = \frac{H_{max}}{U_{gas}} \qquad (3)$$

where H_{max} is the maximum height of the foam and U_{gas} is the gas flow rate, while the foam production, f_P, is calculated as [56]:

$$f_P = \frac{\Sigma}{U_D} \qquad (4)$$

where U_D is the average rate of foam decay.

2.2.4. Dynamic Fluid-Film Interferometry

The thinning dynamics of the foam thin film formed between the colliding bubble and the free surface was monitored using the Dynamic Fluid-Film Interferometer (DFI) shown in Figure 1. The bubble was formed at the capillary orifice of inner diameter 0.051 mm mounted at the bottom of the round glass column. The equivalent diameter of the bubble (d_{eq}) detaching from the capillary was 1.31 ± 0.02 mm in distilled water. The time delay between two successive bubbles was equal to at least 60 s and was adjusted using a precise 'bubble-on-demand' generator [57]. The distance (L) covered by the bubble from the moment of its release to the moment of liquid film formation was equal to 1.0 or 10 cm. The interference patterns were acquired using top-view camera UI-3280CP-C-HQ (IDS Imaging Development Systems GmbH, Obersulm, Germany) equipped with a light source LAV-80SW2 (CCS Inc., Kyoto, Japan), Zoom Imaging Lens VZM450 (Edmund Optics, Barrington, NJ, USA), and a tri-band filter Edmund Optics #87245 with pass bands at 457 nm, 530 nm, and 628 nm. The film thickness was obtained by analysis of the reflection interference data, i.e., by mapping the colors in the recorded videos, using the classical light intensity–film thickness relationship described in detail in refs. [58,59].
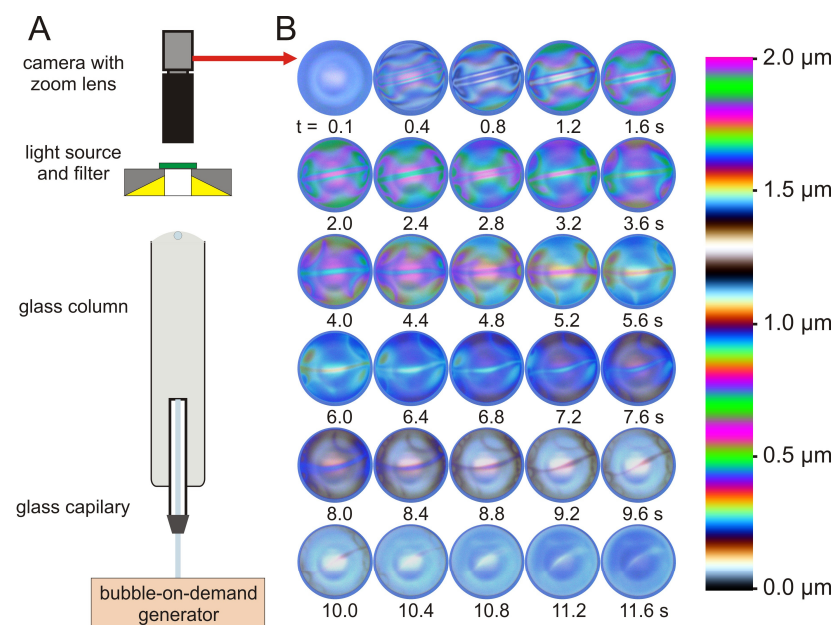
Figure 1. (**A**) Schematic view of the Dynamic Fluid-Film Interferometer and (**B**) sequence of experimentally acquired DFI images of a foam film formed at $L = 1.0$ cm for $c_{LAE} = 253$ mg/dm^3 and $c_{PGA} = 100$ mg/dm^3.

All experiments were carried out at room temperature of 21 ± 3 °C.

3. Results and Discussion

3.1. Physicochemical Characterization of Polyelectrolytes

Figure 2 presents the bulk physicochemical properties of the studied polyelectrolytes. The results in Figure 2A show that at pH 5.8, the electrokinetic potential remains highly positive for PLL and highly negative for PGA, with only slight changes as ionic strength increases. These results indicate that both polyelectrolytes are highly charged, which affects their conformation. Indeed, the hydrodynamic diameter shown in Figure 2B suggests that both macromolecules exhibit a rather elongated conformation [60,61], which may influence the mechanism of foam stabilization.
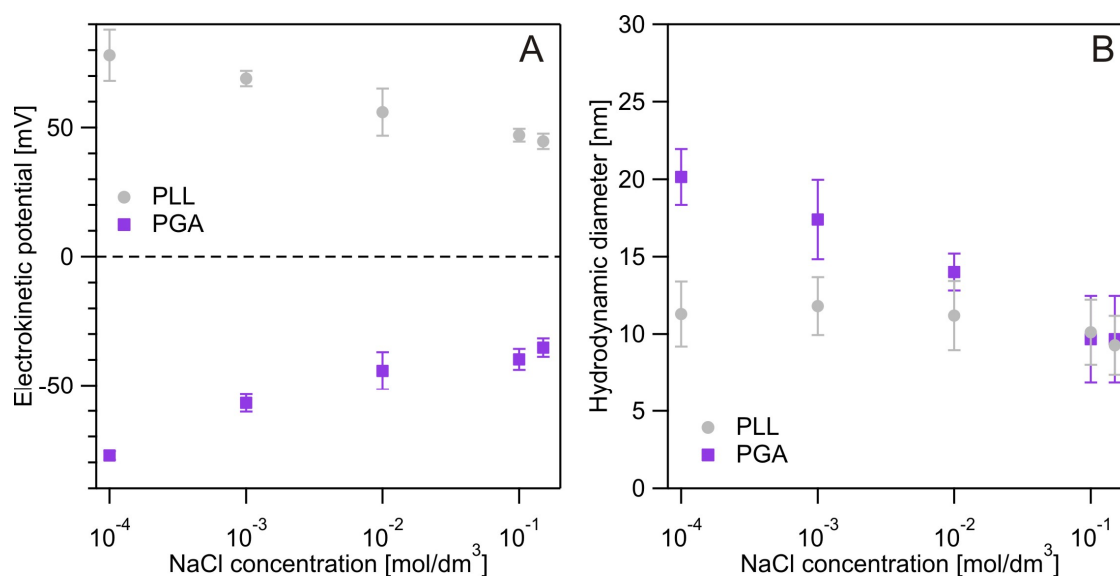

Figure 2. (**A**) Electrokinetic potential and (**B**) hydrodynamic diameter of poly-L-lysine and poly-L-glutamic acid in function of NaCl concentration in pH 5.8.

3.2. Surface Tension Measurements

The basic information about the interaction between the surfactant and oppositely charged polyelectrolyte was obtained from surface tension measurements. Figure 3A,B show the surface tension as a function of surfactant concentration for PGA/LAE and PLL/RH compositions, respectively. In both cases, the polyelectrolyte concentration was 100 mg/dm^3. Additionally, data for surfactants without polyelectrolytes are presented. This polyelectrolyte concentration was chosen after a series of preliminary measurements, which showed it to be optimal. At lower PE concentrations, the effect of the added polyelectrolyte was imperceptible, or a second phase appeared in the bulk, significantly reducing the concentration range in which the study could be conducted. On the other hand, higher PE concentrations led to significantly increased research costs without notable improvements in foam stability. It is worth mentioning that polypeptides alone have no adsorption properties at the water/air interface [62,63].

The critical micelle concentration was found to be ca. 94 mg/dm^3 and 46 mg/dm^3 for LAE and RH, respectively, which is in good agreement with the literature data [45,52]. As seen in both figures, the addition of polyelectrolyte caused a decrease in surface tension compared to the pure surfactant solution. This effect is more pronounced at low-to-intermediate concentrations, while at higher concentrations, the effect diminishes, leading to a slight increase compared to the pure surfactant solution. The observed decrease can be related to two effects: (i) presence of polyelectrolytes can influence the adsorption coverage of ionic surfactant over the liquid/gas interface and/or (ii) polymer/surfactant complexes were formed on the liquid/gas interface [64–66]. In both cases, measurements were concluded at the concentration where a second phase appeared, as indicated by a significant increase in

the measured surface tension meaning that polyelectrolyte/surfactant complexes desorb, resulting in reduced adsorption of surfactant at the interface [64,67].
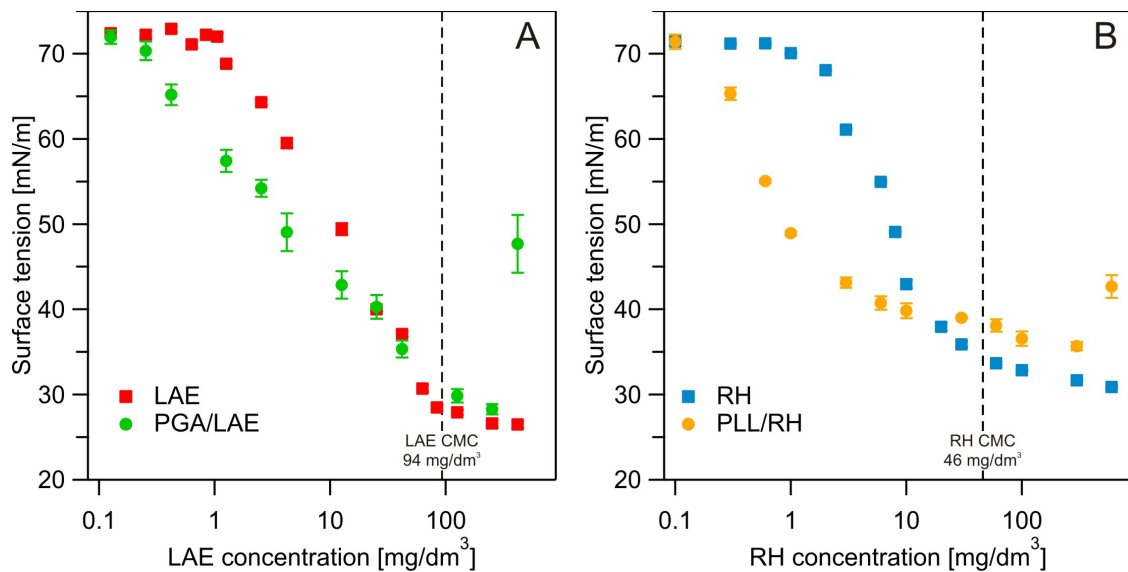

Figure 3. Surface tension of (**A**) pure LAE and PGA/LAE mixture and (**B**) RH and PLL/RH mixture in function of surfactant concentration. PGA and PLL concentrations were 100 mg/dm^3.

3.3. Dynamic Foam Analysis

While surface tension measurement is an excellent tool for studying the behavior of surface-active substances at the fluid interface and the mechanism of adsorption, the investigation of foams often requires different techniques. For this purpose, dynamic foam analysis is an effective method for evaluating foamability and foam decay. This technique provides quantitative information, such as foam height and the rate of foam decay. Both parameters can be further used to calculate the Bikerman unit of foaminess [55] and the foam production [56], which are interchangeable measures of foamability.

Figures 4 and 5 present foam height as a function of time for PGA/LAE and PLL/RH compositions, respectively, at various surfactant concentrations. In all measurements, the first 20 s was the stage during which air was pumped and the foam was formed, reaching its maximum height at the end of this period. Once the air pumping was stopped, foam decay began, and in most cases, the foam disappeared within 100 s.
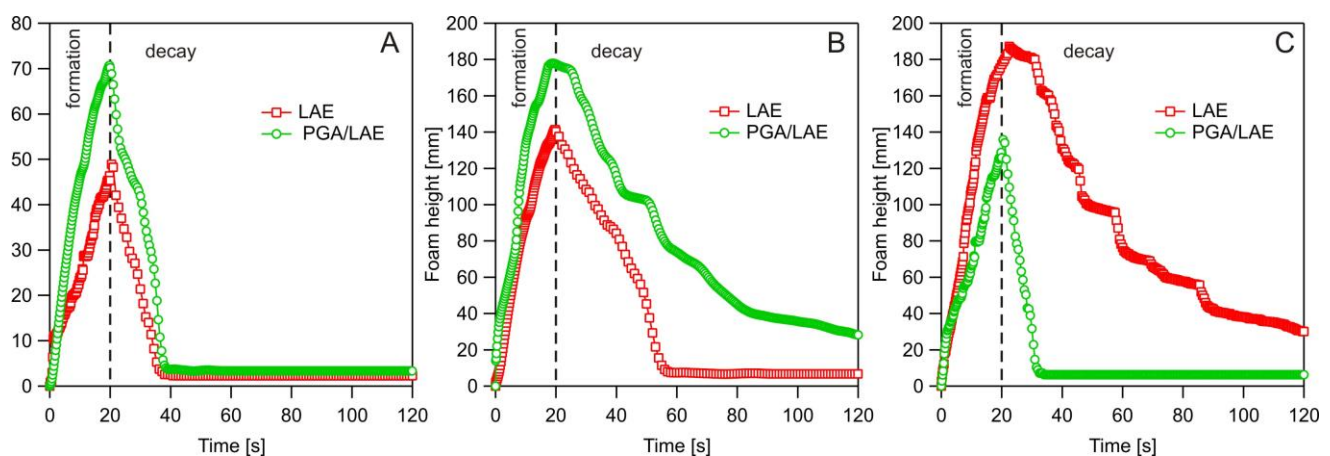
Figure 4. Foamability and foam decay for pure LAE and PGA/LAE mixture for (**A**) c_{LAE} = 42.1 mg/dm^3, (**B**) c_{LAE} = 253 mg/dm^3, and (**C**) c_{LAE} = 421 mg/dm^3. PGA concentration was 100 mg/dm^3.
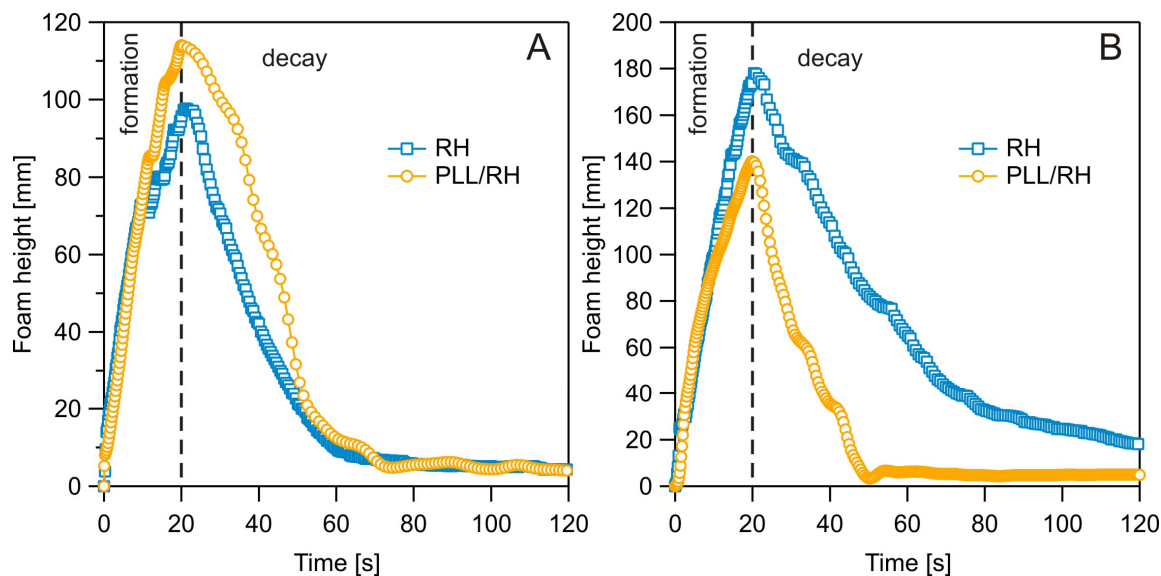
Figure 5. Foamability and foam decay for RH and PLL/RH mixture for (**A**) c_{RH} = 100 mg/dm^3 and (**B**) c_{RH} = 600 mg/dm^3. PLL concentration was 100 mg/dm^3.

In the case of the PGA/LAE system, the presence of polyelectrolyte increased the maximum foam height (H_{max}) and slowed down foam decay compared to the pure surfactant. At the highest studied concentration, a substantial decrease in both foam height and stability was observed, which correlates well with the surface tension data. A similar qualitative effect of increased maximum foam height was observed for the PLL/RH compositions and at the highest concentration, both parameters deteriorated significantly. When it comes to foam stability, it showed no significant improvement—for both, pure surfactant and its mixture with polyelectrolyte, sharp foam decay was observed.

To our surprise, the PGA/LAE composition exhibited better foaming properties than PLL/RH, which is contrary to the data from the surface tension measurements. Therefore, for a thorough quantitative analysis, the Bikerman foaminess and the foam production were determined across the entire range of studied surfactant concentrations. The gas flow was the same through all measurements; thus, the calculated values of Bikerman foaminess are directly proportional to the maximum foam heights. In case of the foam production, this parameter is a result of two effects: foaminess and foam decay.

The calculated values of both parameters are presented in Figures 6 and 7 for the PGA/LAE and PLL/RH systems, respectively. In both systems, at low surfactant concentrations, there was no difference between the surfactant alone and the polyelectrolyte/surfactant composition, even though surface tension measurements showed a clear effect on macromolecules. The effect of polyelectrolyte addition was observed in the concentration range where the pure surfactant solution also showed increased foaminess. The increase in foamability of the studied solutions was noted starting at concentrations close to the CMC of the pure surfactant.

The data in Figure 6A,B show that poly-L-glutamic acid had a synergistic effect when mixed with ethyl lauroyl arginate. For the surfactant alone, both parameters describing foam formation and stability increased with surfactant concentration starting at the CMC. The addition of PGA further improved foaminess, but at the highest LAE concentration, a second phase precipitated. This phenomenon had a moderate influence on the maximum foam height, but it caused rapid foam decay and decomposition within 20 s, as shown in Figure 4C. This effect was consistent with the observations made during surface tension measurements, where the surface tension increased once precipitates appeared in the solution. Thus, the removal of surfactants and PE/S complexes from the liquid/air interfaces resulted in decreased foam stability and rapid foam decay.
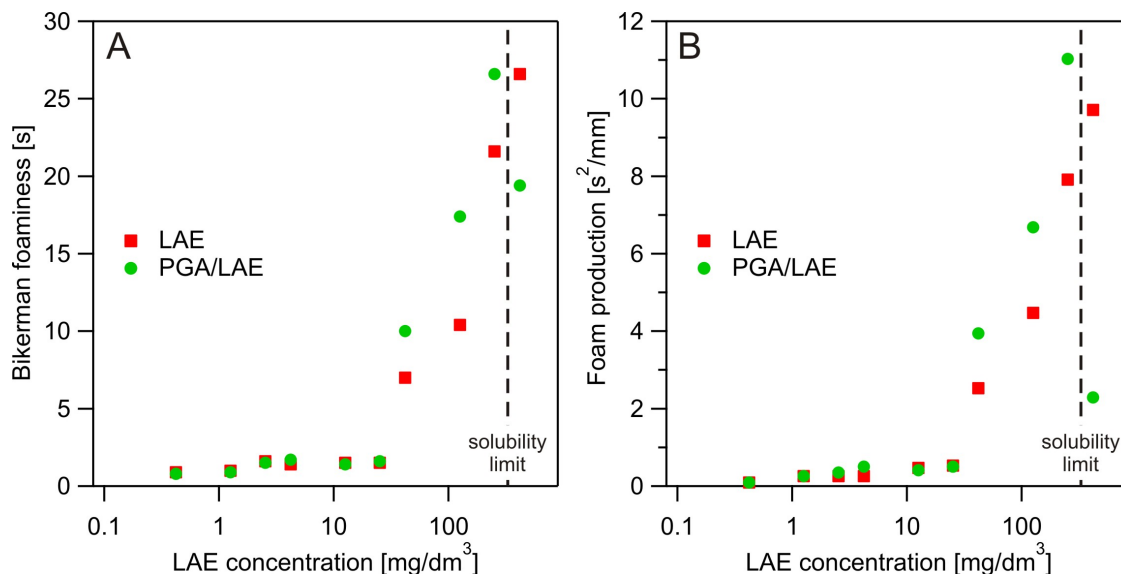
Figure 6. (**A**) Bikerman foaminess and (**B**) foam production for pure LAE and PGA/LAE mixture in function of surfactant concentration. PGA concentration was 100 mg/dm^3.
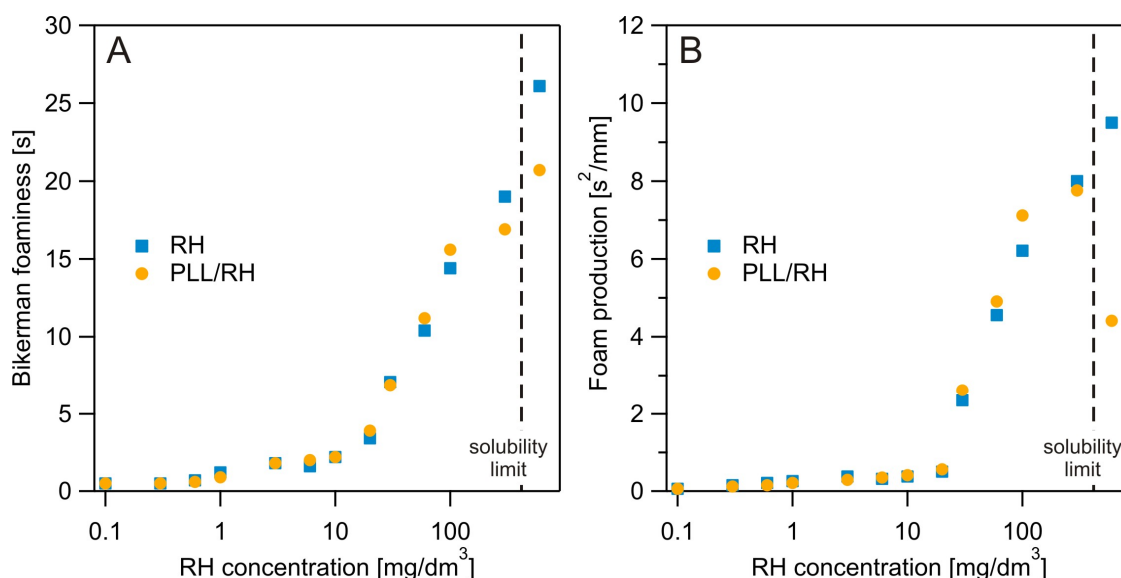
Figure 7. (**A**) Bikerman foaminess and (**B**) foam production for RH and PLL/RH mixture in function of surfactant concentration. PLL concentration was 100 mg/dm^3.

The results for Bikerman foaminess and foam production for RH alone and the PLL/RH mixture are presented in Figure 7A,B. Similar to ethyl lauroyl arginate, rhamnolipids alone showed an increase in both parameters with increasing surfactant concentration, starting at the CMC. Additionally, both surfactants, LAE and RH, exhibited similar properties regarding maximum foam height and foam decay rate within a comparable concentration range. However, there was a slight shift toward lower concentrations for rhamnolipids, which can be correlated with their CMC values.

As previously mentioned, the addition of PLL to rhamnolipids had an insignificant impact on foam formation and stability. This result might seem surprising in light of the surface tension measurements, but it is important to note that stable foam is typically obtained at surfactant concentrations above the CMC.

The limited effectiveness of PLL in the PLL/RH composition is likely related to the ionic nature of rhamnolipids. As reported in the literature [44,45], at pH 5.8, rhamnolipids exhibit rather weak ionic/non-ionic properties. Therefore, additional measurements were

conducted at pH 10, where the dominant form of rhamnolipids is ionic due to the deprotonation of the carboxylic group [68]. It should be noted that the electrokinetic potential of PLL at pH 10 and 1×10^{-4} mol/dm^3 NaCl concentration exhibits a strongly positive value equal to 62 mV. The foam production increased from 2.6 s^2/mm at pH 5.8 to 4.3 s^2/mm at pH 10, and from 4.9 s^2/mm at pH 5.8 to 6.1 s^2/mm at pH 10 for rhamnolipids concentrations of 30 mg/dm^3 and 60 mg/dm^3, respectively. These data highlight the importance of pH on the foaminess properties of the PLL/RH system.

For a better analysis of the relation between surface tension and foamability, the foam production as a function of surface tension for all studied systems is presented in Figure 8. It shows that a decrease in surface tension below 40 mN/m caused a sharp increase in foam stability. Interestingly, for pure surfactant solutions above the CMC, foam production increased even though surface tension changed only slightly. The effect of micelles on foam stability and drainage is well known in the literature, but it is not unequivocal, ranging from increased stability to no influence and even decreased foaminess [69–72]. In our case, further increases in surfactant concentration above the CMC had a positive effect on foam stability. While the exact mechanism is unclear, this may be related to the charge of surfactant, which also formed charged micelles. The presence of electrostatic interactions likely slowed the drainage of the thin liquid films in the foam lamellae. In the case of polyelectrolyte addition, foams produced from the PE/S mixture exhibited better foaminess than those from pure surfactant at similar surface tensions. The PE/S complexes were likely less charged than micelles, as the ionic groups were neutralized by the oppositely charged components of the mixture. This suggests that, for PE/S complexes, another mechanism was responsible for the improvement in foam stability. Since the polyelectrolytes used are macromolecules, steric repulsion from the polymer chains could be responsible for the increased foam stability [73–75].
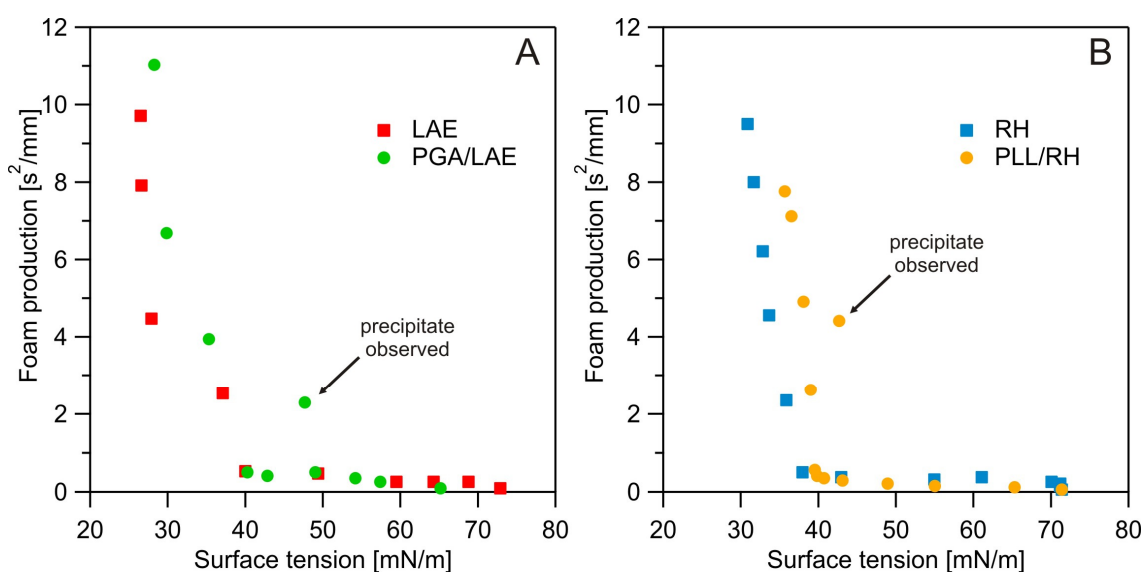
Figure 8. Foam production of (**A**) pure LAE and PGA/LAE mixture and (**B**) RH and PLL/RH mixture in function of surface tension. PGA and PLL concentrations were 100 mg/dm^3.

Even in mixtures where precipitates were observed, foam production is greater for a PE/S mixture than for a pure surfactant solution with the same surface tension. This phenomenon might be directly related to the presence of interfacial aggregates. Therefore, surface tension is not a very accurate indicator of foaminess for either the PGA/LAE or PLL/RH systems. Additional factors, such as the rheology of interfacial surfaces and thin liquid films, may be necessary to obtain a more comprehensive understanding of the foamability of the studied compositions [24,76,77].

3.4. Dynamic Fluid-Film Interferometry

To gain a more comprehensive understanding of the foaminess properties of the studied polyelectrolyte/surfactant compositions, Dynamic Fluid-Film Interferometry (DFI), which allows for the investigation of single foam films, was applied. During a typical DFI experiment, when a rising bubble approached the free surface, a thin liquid film was formed. Due to light reflection at the liquid/air interfaces, colorful patterns were observed, as shown in Figure 1B. These recorded patterns were analyzed to provide information about the lifetime and thinning velocity of the single foam film. Moreover, by adjusting the distance between the point where the bubble was formed and the free surface, various states of the dynamic adsorbed layer (DAL) on the bubble surfaces were obtained [78,79]. Thus, for a 'close' distance, it was expected to have surfactant molecules uniformly distributed over the bubble surface. In contrast, at a 'far' distance, surfactant depletion was expected at the front (upstream) part of the bubble, with accumulation in the rear.

Figure 9A,B show the thin liquid (foam) film (TLF) lifetime as a function of surfactant concentration for PGA/LAE and PLL/RH compositions, respectively, at two different distances. In both cases, three characteristic ranges can be distinguished. The first range occurs at low surfactant concentrations, where the thin liquid film was completely unstable, rupturing almost immediately after its formation. In the intermediate surfactant concentration range, i.e., below the surfactant CMC, the TLF lifetime oscillated around 5 s. In the final range, above the CMC, film stability increased, with TLF lifetimes exceeding 10 s. However, at the highest surfactant concentration, in the presence of polyelectrolyte, a significant decrease in stability was observed.
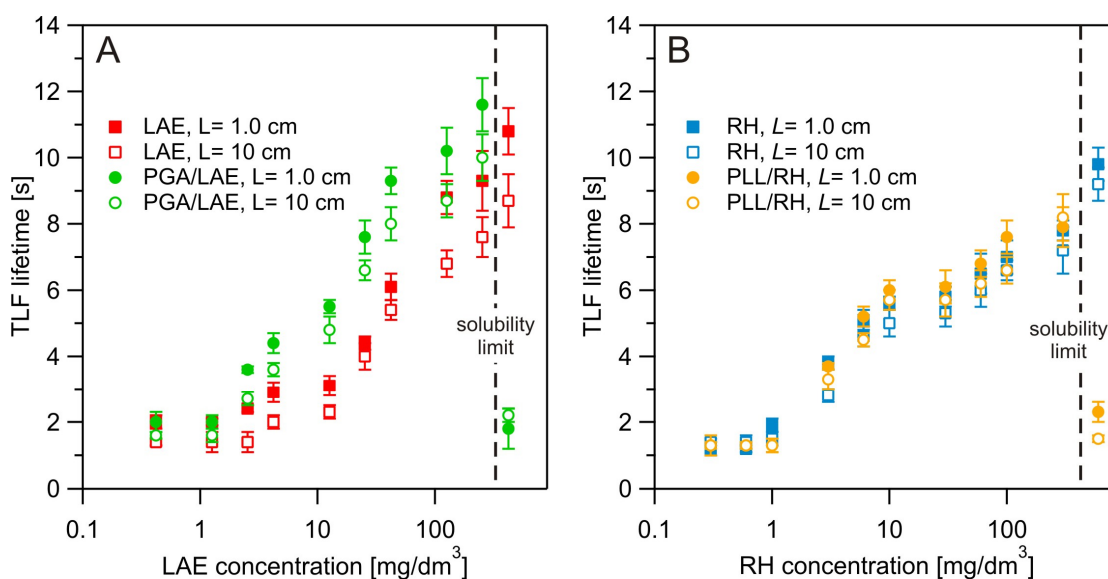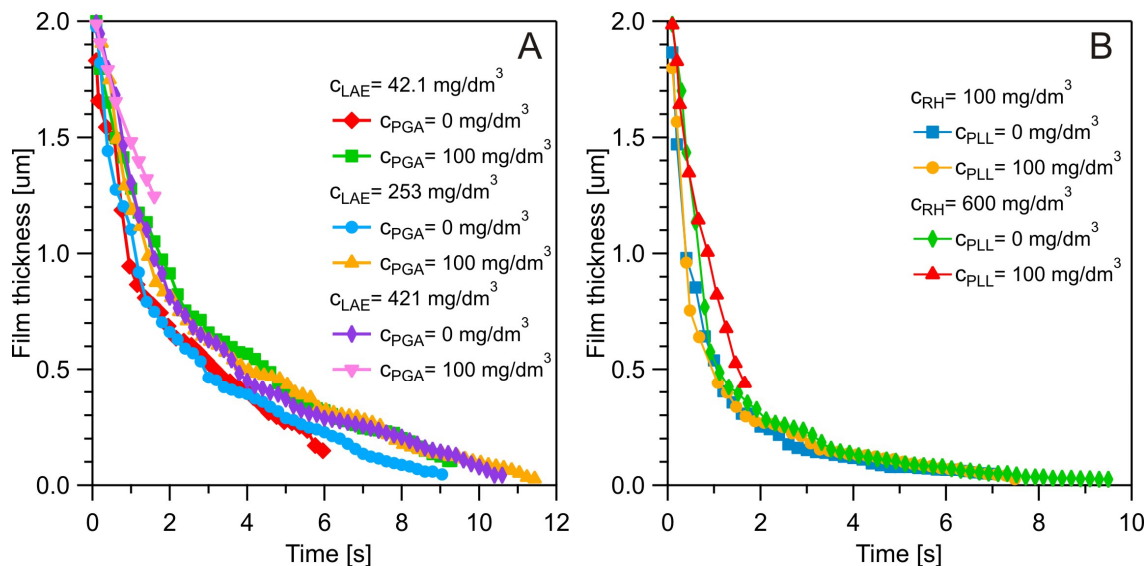

Figure 9. Thin liquid film (TLF) lifetime of (**A**) pure LAE and PGA/LAE mixture and (**B**) RH and PLL/RH mixture in function of surfactant concentration. PGA and PLL concentrations were 100 mg/dm³.

For both the PGA/LAE and PLL/RH systems, the TLF lifetime data show a qualitative similarity to the results obtained from DFA measurements. A noticeable difference in TLF lifetime was observed between PGA/LAE and LAE alone, while the values for PLL/RH and RH alone overlapped. Thus, it can be concluded that the lifetime of a single thin liquid film correlates much better with the foaminess of the studied compounds than surface tension data.

It is interesting to note that the influence of the dynamically adsorbed layer on TLF lifetime was rather insignificant for all studied solutions, as shown in Figure 9. This lack of a 'distance' effect could be attributed to the rapid formation of the DAL over the bubble surface, resulting in similar coverage states on bubbles colliding with the free surface at

both 1 cm and 10 cm. Thus, to investigate the effect of the dynamically adsorbed layer on TLF stability more closely, further measurements at shorter distances or using a 'bubble trap' apparatus are needed [57,80].

In addition to providing information about the lifetime of a thin liquid film, Dynamic Fluid-Film Interferometry also delivers data on film thickness and drainage. Figure 10A,B show the thin liquid (foam) film thickness as a function of time for PGA/LAE and PLL/RH compositions, respectively, at various surfactant concentrations.
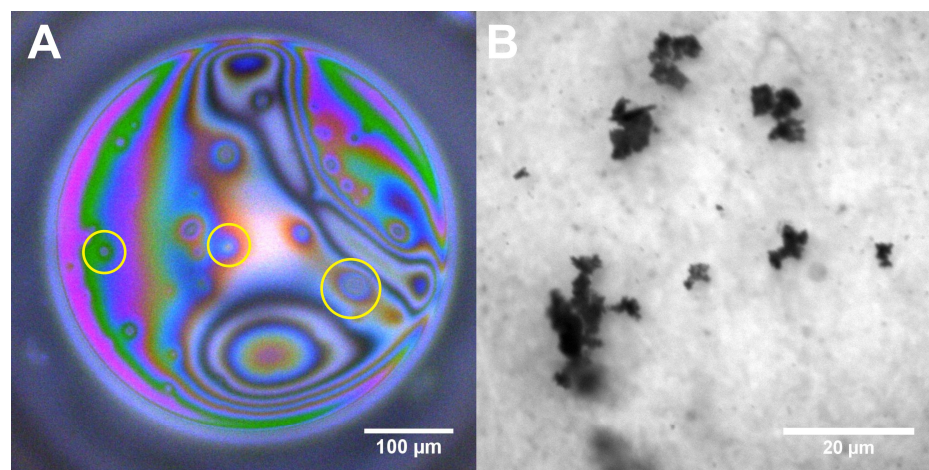

Figure 10. Drainage of the foam film formed at *L* = 1.0 cm of (**A**) pure LAE and PGA/LAE mixture and (**B**) RH and PLL/RH mixture in function of surfactant concentration.

In the case of pure LAE solution, an increase in surfactant concentration showed two effects: (i) initially, it increased film stability, leading to drainage to a thinner critical thickness before rupturing; and (ii) subsequently, it slowed down film drainage, extending the TLF lifetime. The addition of polyelectrolyte further slowed the drainage of the thin liquid film. The critical rupturing thickness was found to be in the range of 30–50 nm for TLFs with lifetimes exceeding 8 s. Once the critical concentration for second-phase precipitation was reached, the thin liquid film ruptured within approximately 2 s at a thickness above 1000 nm. However, even during this short period, a significant slowdown in film drainage was observed.

In the case of the PLL/RH system, the presence of polyelectrolyte did not affect film drainage or the critical thickness at which rupturing occurred. A significant slowdown in TLF drainage was observed only at the highest RH concentration in the presence of PLL, but similar to the PGA/LAE composition, the TLF lifetime remained below 2 s. This significant slowing of film drainage in the polyelectrolyte/surfactant system could be attributed to the bulk rheological properties, as reported in the literature [24]. However, the appearance of a second phase indicated the desorption of polyelectrolyte/surfactant complexes from the liquid/gas interface, which led to a decrease in film stability.

The presence of large polyelectrolyte/surfactant aggregates in the foam film was evident not only through the slowing of drainage and shortening of the lifetime but also by characteristic changes at the film interface. As seen in Figure 11A (highlighted by yellow circles), there are localized formations that were likely large aggregates, similar to those presented in the literature [65]. Unfortunately, the films formed under these conditions were unstable, making a thorough investigation of this phenomenon impossible. In our opinion, this finding requires further research, which could likely be conducted at higher surfactant concentrations to ensure sufficient stability of the thin liquid film. It is worth mentioning that the precipitates observed in the bulk are much bigger than interfacial aggregates (see Figure 11B).

Figure 11. (**A**) DFI photographic image of a foam film containing interfacial microgels formed at $L = 1.0$ cm for $c_{LAE} = 421$ mg/dm^3 and $c_{PGA} = 100$ mg/dm^3. Some of the interfacial aggregates are highlighted by yellow circles (**B**) Microscopic image of aggregates precipitated in a PGA/LAE solution: $c_{LAE} = 421$ mg/dm^3 and $c_{PGA} = 100$ mg/dm^3.

4. Conclusions

As foam systems are crucial for many industrial processes, such as froth flotation, enhanced oil recovery, and flocculation, studying their physicochemical properties, including stability and drainage, is of great interest. To obtain foam with specific and desirable properties, the addition of a surface-active agent is necessary. In this work, foams were produced using *bio*-surfactants, specifically rhamnolipids and ethyl lauroyl arginate, as well as their mixtures with oppositely charged synthetic polypeptides (poly-L-lysine and poly-L-glutamic acid).

Examination of the influence of surfactants alone shows that both compounds exhibit foamability above their CMC. Further increases in concentration led to the production of foams with enhanced stability and reduced foam decay, as confirmed by two independent techniques: dynamic foam analysis and dynamic fluid-film interferometry.

The addition of poly-L-glutamic acid to ethyl lauroyl arginate had a notable impact on foam properties. In terms of foam formation, an increase in maximum foam height and a reduction in the rate of foam decay were observed. These findings were confirmed through the investigation of a single foam film formed under dynamic conditions. The DFI method demonstrated that the presence of PGA prolonged the lifetime of the thin liquid film and resulted in film drainage to thinner critical thicknesses of rupturing.

In the case of the poly-L-lysine/rhamnolipids system, the polyelectrolyte effect was much less significant. This lack of effect was attributed to the primarily non-ionic nature of rhamnolipids molecules at pH 5.8. To examine this hypothesis more thoroughly, preliminary measurements of foam stability for the PLL/RH mixture at pH 10 were conducted. The results showed that the increased charge of the surfactant molecules enhanced the foamability of the studied compositions. Therefore, further investigation into the effect of pH on the foamability of polyelectrolyte/surfactant systems is required.

It should be emphasized that polyelectrolyte/surfactant systems can only be used within a narrow concentration range. Increasing the surfactant concentration while keeping the polyelectrolyte concentration constant caused the formation of a second phase in precipitated form. This phenomenon led to the removal of surfactants and polyelectrolyte/surfactant complexes from the air/water interfaces, resulting in decreased foamability and rapid foam decay.

The presented study demonstrated that polyelectrolyte/surfactant systems could be an interesting and promising alternative to standard foaming formulations. These systems mitigate negative environmental impacts while maintaining efficiency in foam production and stability. However, the preliminary data presented in this study require

further investigation to optimize PE/S compositions. Therefore, additional exploration of the influence of pH and ionic strength on foamability is necessary, as well as an investigation into the critical concentration of coalescence (CCC) and the formation of the dynamic adsorption layer.

Author Contributions: Conceptualization, D.K.; methodology, D.K., A.W.-P., M.M. and J.Z.; software, Ł.W. and J.Z.; investigation, D.K., A.W.-P. and M.M.; analysis and data curation, D.K.; writing—original draft preparation, D.K. and Ł.W.; writing—review and editing, D.K., A.W.-P., M.M., Ł.W. and J.Z.; visualization, D.K.; funding acquisition, D.K. and J.Z. All authors have read and agreed to the published version of the manuscript.

Data Availability Statement: Data will be made available by the authors on request.

Conflicts of Interest: The authors declare no conflicts of interest.

References

1. Cho, Y.S.; Laskowski, J.S. Effect of Flotation Frothers on Bubble Size and Foam Stability. *Int. J. Miner. Process.* **2002**, *64*, 69–80. [CrossRef]
2. Karakashev, S.I.; Grozev, N.A.; Ozdemir, O.; Batjargal, K.; Guven, O.; Ata, S.; Bournival, G.; Boylu, F.; Sabri Çelik, M. On the Frother's Strength and Its Performance. *Miner. Eng.* **2021**, *171*, 107093. [CrossRef]
3. Murray, B.S. Recent Developments in Food Foams. *Curr. Opin. Colloid Interface Sci.* **2020**, *50*, 101394. [CrossRef]
4. Sheng, Y.; Xue, M.; Ma, L.; Zhao, Y.; Wang, Q.; Liu, X. Environmentally Friendly Firefighting Foams Used to Fight Flammable Liquid Fire. *Fire Technol.* **2021**, *57*, 2079–2096. [CrossRef]
5. Schad, T.; Preisig, N.; Drenckhan, W.; Stubenrauch, C. Foam-Based Cleaning of Surfaces Contaminated with Mixtures of Oil and Soot. *J. Surfactants Deterg.* **2022**, *25*, 377–385. [CrossRef]
6. Arzhavitina, A.; Steckel, H. Foams for Pharmaceutical and Cosmetic Application. *Int. J. Pharm.* **2010**, *394*, 1–17. [CrossRef] [PubMed]
7. Fameau, A.-L.; Fujii, S. Stimuli-Responsive Liquid Foams: From Design to Applications. *Curr. Opin. Colloid Interface Sci.* **2020**, *50*, 101380. [CrossRef]
8. Ritacco, H.A. Polyelectrolyte/Surfactant Mixtures: A Pathway to Smart Foams. *ACS Omega* **2022**, *7*, 36117–36136. [CrossRef]
9. Chiappisi, L.; Hoffmann, I.; Gradzielski, M. Complexes of Oppositely Charged Polyelectrolytes and Surfactants—Recent Developments in the Field of Biologically Derived Polyelectrolytes. *Soft Matter* **2013**, *9*, 3896–3909. [CrossRef]
10. Martinelli, H.; Domínguez, C.; Leyes, M.F.; Moya, S.; Ritacco, H. A pH-Responsive Foam Formulated with PAA/Gemini 12-2-12 Complexes. *Colloids Interfaces* **2021**, *5*, 37. [CrossRef]
11. Babaev, M.S.; Lobov, A.N.; Shishlov, N.M.; Kolesov, S.V. pH-Sensitive Particles of Polymer-Surfactant Complexes Based on a Copolymer of N,N′-Diallyl-N,N′-Dimethylammonium Chloride with Maleic Acid and Sodium Dodecyl Sulfate. *React. Funct. Polym.* **2022**, *178*, 105359. [CrossRef]
12. Benhur, A.M.; Diaz, J.; Amin, S. Impact of Polyelectrolyte-Surfactant Interactions on the Rheology and Wet Lubrication Performance of Conditioning Shampoo. *Int. J. Cosmet. Sci.* **2021**, *43*, 246–253. [CrossRef]
13. Schnurbus, M.; Hardt, M.; Steinforth, P.; Carrascosa-Tejedor, J.; Winnall, S.; Gutfreund, P.; Schönhoff, M.; Campbell, R.A.; Braunschweig, B. Responsive Material and Interfacial Properties through Remote Control of Polyelectrolyte–Surfactant Mixtures. *ACS Appl. Mater. Interfaces* **2022**, *14*, 4656–4667. [CrossRef] [PubMed]
14. Alter, H. The Recovery of Plastics from Waste with Reference to Froth Flotation. *Resour. Conserv. Recycl.* **2005**, *43*, 119–132. [CrossRef]
15. Peleka, E.N.; Gallios, G.P.; Matis, K.A. A Perspective on Flotation: A Review. *J. Chem. Technol. Biotechnol.* **2018**, *93*, 615–623. [CrossRef]
16. Barany, S.; Szepesszentgyörgyi, A. Flocculation of Cellular Suspensions by Polyelectrolytes. *Adv. Colloid Interface Sci.* **2004**, *111*, 117–129. [CrossRef] [PubMed]
17. Bournival, G.; Du, Z.; Ata, S.; Jameson, G.J. Foaming and Gas Dispersion Properties of Non-Ionic Frothers in the Presence of Hydrophobized Submicron Particles. *Int. J. Miner. Process.* **2014**, *133*, 123–131. [CrossRef]
18. Eftekhari, M.; Schwarzenberger, K.; Karakashev, S.I.; Grozev, N.A.; Eckert, K. Oppositely Charged Surfactants and Nanoparticles at the Air-Water Interface: Influence of Surfactant to Nanoparticle Ratio. *J. Colloid Interface Sci.* **2024**, *653*, 1388–1401. [CrossRef]
19. Kristen, N.; von Klitzing, R. Effect of Polyelectrolyte/Surfactant Combinations on the Stability of Foam Films. *Soft Matter* **2010**, *6*, 849–861. [CrossRef]
20. Chronakis, I.S.; Alexandridis, P. Rheological Properties of Oppositely Charged Polyelectrolyte−Surfactant Mixtures: Effect of Polymer Molecular Weight and Surfactant Architecture. *Macromolecules* **2001**, *34*, 5005–5018. [CrossRef]

21. Langevin, D. Polyelectrolyte and Surfactant Mixed Solutions. Behavior at Surfaces and in Thin Films. *Adv. Colloid Interface Sci.* **2001**, *89–90*, 467–484. [CrossRef] [PubMed]

22. Kleinschmidt, F.; Stubenrauch, C.; Delacotte, J.; von Klitzing, R.; Langevin, D. Stratification of Foam Films Containing Polyelectrolytes. Influence of the Polymer Backbone's Rigidity. *J. Phys. Chem. B* **2009**, *113*, 3972–3980. [CrossRef] [PubMed]

23. Petkova, R.; Tcholakova, S.; Denkov, N.D. Foaming and Foam Stability for Mixed Polymer–Surfactant Solutions: Effects of Surfactant Type and Polymer Charge. *Langmuir* **2012**, *28*, 4996–5009. [CrossRef] [PubMed]

24. Braun, L.; von Klitzing, R. When Bulk Matters: Disentanglement of the Role of Polyelectrolyte/Surfactant Complexes at Surfaces and in the Bulk of Foam Films. *Langmuir* **2023**, *39*, 111–118. [CrossRef]

25. Pereira, J.L.; Vidal, T.; Gonçalves, F.J.M.; Gabriel, R.G.; Costa, R.; Rasteiro, M.G. Is the Aquatic Toxicity of Cationic Polyelectrolytes Predictable from Selected Physical Properties? *Chemosphere* **2018**, *202*, 145–153. [CrossRef]

26. Arora, J.; Ranjan, A.; Chauhan, A.; Biswas, R.; Rajput, V.D.; Sushkova, S.; Mandzhieva, S.; Minkina, T.; Jindal, T. Surfactant Pollution, an Emerging Threat to Ecosystem: Approaches for Effective Bacterial Degradation. *J. Appl. Microbiol.* **2022**, *133*, 1229–1244. [CrossRef]

27. Drzymala, J.; Kowalczuk, P.B. Classification of Flotation Frothers. *Minerals* **2018**, *8*, 53. [CrossRef]

28. Pawliszak, P.; Bradshaw-Hajek, B.H.; Skinner, W.; Beattie, D.A.; Krasowska, M. Frothers in Flotation: A Review of Performance and Function in the Context of Chemical Classification. *Miner. Eng.* **2024**, *207*, 108567. [CrossRef]

29. Rao, F.; Liu, Q. Froth Treatment in Athabasca Oil Sands Bitumen Recovery Process: A Review. *Energy Fuels* **2013**, *27*, 7199–7207. [CrossRef]

30. Sun, Q.; Li, Z.; Li, S.; Jiang, L.; Wang, J.; Wang, P. Utilization of Surfactant-Stabilized Foam for Enhanced Oil Recovery by Adding Nanoparticles. *Energy Fuels* **2014**, *28*, 2384–2394. [CrossRef]

31. Gayathiri, E.; Prakash, P.; Karmegam, N.; Varjani, S.; Awasthi, M.K.; Ravindran, B. Biosurfactants: Potential and Eco-Friendly Material for Sustainable Agriculture and Environmental Safety—A Review. *Agronomy* **2022**, *12*, 662. [CrossRef]

32. Nagtode, V.S.; Cardoza, C.; Yasin, H.K.A.; Mali, S.N.; Tambe, S.M.; Roy, P.; Singh, K.; Goel, A.; Amin, P.D.; Thorat, B.R.; et al. Green Surfactants (Biosurfactants): A Petroleum-Free Substitute for Sustainability—Comparison, Applications, Market, and Future Prospects. *ACS Omega* **2023**, *8*, 11674–11699. [CrossRef] [PubMed]

33. Simões, C.R.; da Silva, M.W.P.; de Souza, R.F.M.; Hacha, R.R.; Merma, A.G.; Torem, M.L.; Silvas, F.P.C. Biosurfactants: An Overview of Their Properties, Production, and Application in Mineral Flotation. *Resources* **2024**, *13*, 81. [CrossRef]

34. Khoshdast, H.; Sam, A.; Vali, H.; Noghabi, K.A. Effect of Rhamnolipid Biosurfactants on Performance of Coal and Mineral Flotation. *Int. Biodeter. Biodegrad.* **2011**, *65*, 1238–1243. [CrossRef]

35. Chernyshova, I.; Slabov, V.; Kota, H.R. Emerging Application of Biosurfactants in Metal Extraction. *Curr. Opin. Colloid Interface Sci.* **2023**, *68*, 101763. [CrossRef]

36. Oulkhir, A.; Lyamlouli, K.; Danouche, M.; Ouazzani, J.; Benhida, R. A Critical Review on Natural Surfactants and Their Potential for Sustainable Mineral Flotation. *Rev. Environ. Sci. Biotechnol.* **2023**, *22*, 105–131. [CrossRef]

37. Xi, W.; Ping, Y.; Alikhani, M.A. A Review on Biosurfactant Applications in the Petroleum Industry. *Int. J. Chem. Eng.* **2021**, *2021*, 5477185. [CrossRef]

38. Paul, I.; Mandal, T.; Mandal, D.D. Assessment of Bacterial Biosurfactant Production and Application in Enhanced Oil Recovery (EOR)—A Green Approach. *Environ. Technol. Innov.* **2022**, *28*, 102733. [CrossRef]

39. Souza, E.C.; Vessoni-Penna, T.C.; de Souza Oliveira, R.P. Biosurfactant-Enhanced Hydrocarbon Bioremediation: An Overview. *Int. Biodeter. Biodegrad.* **2014**, *89*, 88–94. [CrossRef]

40. Malkapuram, S.T.; Sharma, V.; Gumfekar, S.P.; Sonawane, S.; Sonawane, S.; Boczkaj, G.; Seepana, M.M. A Review on Recent Advances in the Application of Biosurfactants in Wastewater Treatment. *Sustain. Energy Technol. Assess.* **2021**, *48*, 101576. [CrossRef]

41. Deming, T.J. Synthetic Polypeptides for Biomedical Applications. *Prog. Polym. Sci.* **2007**, *32*, 858–875. [CrossRef]

42. Bajaj, I.; Singhal, R. Poly (Glutamic Acid)—An Emerging Biopolymer of Commercial Interest. *Bioresour. Technol.* **2011**, *102*, 5551–5561. [CrossRef] [PubMed]

43. Guzmán, E.; Ortega, F.; Rubio, R.G. Exploring the World of Rhamnolipids: A Critical Review of Their Production, Interfacial Properties, and Potential Application. *Curr. Opin. Colloid Interface Sci.* **2024**, *69*, 101780. [CrossRef]

44. Özdemir, G.; Peker, S.; Helvaci, S.S. Effect of pH on the Surface and Interfacial Behavior of Rhamnolipids R1 and R2. *Colloids Surf. A Physicochem. Eng. Asp.* **2004**, *234*, 135–143. [CrossRef]

45. Legawiec, K.J.; Kruszelnicki, M.; Zawadzka, M.; Basařová, P.; Zawala, J.; Polowczyk, I. Towards Green Flotation: Investigating the Effect of Rhamnolipid Biosurfactant on Single Bubble Adhesion Dynamics. *J. Mol. Liq.* **2023**, *388*, 122759. [CrossRef]

46. Khoshdast, H.; Abbasi, H.; Sam, A.; Noghabi, K.A. Frothability and Surface Behavior of a Rhamnolipid Biosurfactant Produced by Pseudomonas Aeruginosa MA01. *Biochem. Eng. J.* **2012**, *60*, 127–134. [CrossRef]

47. Amani, H.; Müller, M.M.; Syldatk, C.; Hausmann, R. Production of Microbial Rhamnolipid by Pseudomonas Aeruginosa MM1011 for Ex Situ Enhanced Oil Recovery. *Appl. Biochem. Biotechnol.* **2013**, *170*, 1080–1093. [CrossRef]

48. Infante, R.; Dominguez, J.G.; Erra, P.; Julia, R.; Prats, M. Surface Active Molecules: Preparation and Properties of Long Chain Nα-Acyl-l-α-Amino-ω-Guanidine Alkyl Acid Derivatives. *Int. J. Cosmet. Sci.* **1984**, *6*, 275–282. [CrossRef]

49. Becerril, R.; Manso, S.; Nerin, C.; Gómez-Lus, R. Antimicrobial Activity of Lauroyl Arginate Ethyl (LAE), against Selected Food-Borne Bacteria. *Food Control* **2013**, *32*, 404–408. [CrossRef]

50. Chi, K.; Catchmark, J.M. Crystalline Nanocellulose/Lauric Arginate Complexes. *Carbohydr. Polym.* **2017**, *175*, 320–329. [CrossRef]

51. Czakaj, A.; Chatzigiannakis, E.; Vermant, J.; Krzan, M.; Warszyński, P. The Influence of the Surface Chemistry of Cellulose Nanocrystals on Ethyl Lauroyl Arginate Foam Stability. *Polymers* **2022**, *14*, 5402. [CrossRef] [PubMed]

52. Czakaj, A.; Jarek, E.; Krzan, M.; Warszyński, P. Ethyl Lauroyl Arginate, an Inherently Multicomponent Surfactant System. *Molecules* **2021**, *26*, 5894. [CrossRef] [PubMed]

53. Russel, W.B.; Saville, D.A.; Schowalter, W.R. *Colloidal Dispersions*; Cambridge Monographs on Mechanics; Cambridge University Press: Cambridge, UK, 1989; ISBN 978-0-521-42600-8.

54. Batjargal, K.; Guven, O.; Ozdemir, O.; Karakashev, S.I.; Grozev, N.A.; Boylu, F.; Çelik, M.S. Frothing Performance of Frother-Collector Mixtures as Determined by Dynamic Foam Analyzer and Its Implications in Flotation. *Minerals* **2023**, *13*, 242. [CrossRef]

55. Bikerman, J.J. The Unit of Foaminess. *Trans. Faraday Soc.* **1938**, *34*, 634–638. [CrossRef]

56. Karakashev, S.I.; Georgiev, P.; Balashev, K. Foam Production—Ratio between Foaminess and Rate of Foam Decay. *J. Colloid Interface Sci.* **2012**, *379*, 144–147. [CrossRef]

57. Zawala, J.; Niecikowska, A. "Bubble-on-Demand" Generator with Precise Adsorption Time Control. *Rev. Sci. Instrum.* **2017**, *88*, 095106. [CrossRef]

58. Kitagawa, K. Thin-Film Thickness Profile Measurement by Three-Wavelength Interference Color Analysis. *Appl. Opt.* **2013**, *52*, 1998–2007. [CrossRef]

59. Chandran Suja, V.; Sentmanat, J.; Hofmann, G.; Scales, C.; Fuller, G.G. Hyperspectral Imaging for Dynamic Thin Film Interferometry. *Sci. Rep.* **2020**, *10*, 11378. [CrossRef]

60. Adamczyk, Z.; Morga, M.; Kosior, D.; Batys, P. Conformations of Poly-l-Lysine Molecules in Electrolyte Solutions: Modeling and Experimental Measurements. *J. Phys. Chem. C* **2018**, *122*, 23180–23190. [CrossRef]

61. Morga, M.; Batys, P.; Kosior, D.; Bonarek, P.; Adamczyk, Z. Poly-L-Arginine Molecule Properties in Simple Electrolytes: Molecular Dynamic Modeling and Experiments. *Int. J. Environ. Res. Public Health* **2022**, *19*, 3588. [CrossRef]

62. Buckingham, J.H.; Lucassen, J.; Hollway, F. Surface Properties of Mixed Solutions of Poly-l-Lysine and Sodium Dodecyl Sulfate: I. Equilibrium Surface Properties. *J. Colloid Interface Sci.* **1978**, *67*, 423–431. [CrossRef]

63. Okubo, T.; Kobayashi, K. Surface Tension of Biological Polyelectrolyte Solutions. *J. Colloid Interface Sci.* **1998**, *205*, 433–442. [CrossRef] [PubMed]

64. Staples, E.; Tucker, I.; Penfold, J.; Warren, N.; Thomas, R.K. Organization of Polymer−Surfactant Mixtures at the Air−Water Interface: Poly(Dimethyldiallylammonium Chloride), Sodium Dodecyl Sulfate, and Hexaethylene Glycol Monododecyl Ether. *Langmuir* **2002**, *18*, 5139–5146. [CrossRef]

65. Monteux, C.; Williams, C.E.; Meunier, J.; Anthony, O.; Bergeron, V. Adsorption of Oppositely Charged Polyelectrolyte/Surfactant Complexes at the Air/Water Interface: Formation of Interfacial Gels. *Langmuir* **2004**, *20*, 57–63. [CrossRef] [PubMed]

66. Penfold, J.; Thomas, R.K.; Taylor, D.J.F. Polyelectrolyte/Surfactant Mixtures at the Air–Solution Interface. *Curr. Opin. Colloid Interface Sci.* **2006**, *11*, 337–344. [CrossRef]

67. Campbell, R.A.; Angus-Smyth, A.; Yanez Arteta, M.; Tonigold, K.; Nylander, T.; Varga, I. New Perspective on the Cliff Edge Peak in the Surface Tension of Oppositely Charged Polyelectrolyte/Surfactant Mixtures. *J. Phys. Chem. Lett.* **2010**, *1*, 3021–3026. [CrossRef]

68. Abbasi, H.; Noghabi, K.A.; Hamedi, M.M.; Zahiri, H.S.; Moosavi-Movahedi, A.A.; Amanlou, M.; Teruel, J.A.; Ortiz, A. Physicochemical Characterization of a Monorhamnolipid Secreted by Pseudomonas Aeruginosa MA01 in Aqueous Media. An Experimental and Molecular Dynamics Study. *Colloids Surf. B Biointerfaces* **2013**, *101*, 256–265. [CrossRef]

69. Carey, E.; Stubenrauch, C. Properties of Aqueous Foams Stabilized by Dodecyltrimethylammonium Bromide. *J. Colloid Interface Sci.* **2009**, *333*, 619–627. [CrossRef]

70. Anachkov, S.E.; Danov, K.D.; Basheva, E.S.; Kralchevsky, P.A.; Ananthapadmanabhan, K.P. Determination of the Aggregation Number and Charge of Ionic Surfactant Micelles from the Stepwise Thinning of Foam Films. *Adv. Colloid Interface Sci.* **2012**, *183–184*, 55–67. [CrossRef]

71. Lee, J.; Nikolov, A.; Wasan, D. Foam Stability: The Importance of Film Size and the Micellar Structuring Phenomenon. *Can. J. Chem. Eng.* **2014**, *92*, 2039–2045. [CrossRef]

72. Wang, H.; Li, J.; Wang, Z.; Wang, D.; Zhan, H. Experimental Investigation of the Mechanism of Foaming Agent Concentration Affecting Foam Stability. *J. Surfactants Deterg.* **2017**, *20*, 1443–1451. [CrossRef]

73. Sedev, R.; Exerowa, D. DLVO and Non-DLVO Surface Forces in Foam Films from Amphiphilic Block Copolymers. *Adv. Colloid Interface Sci.* **1999**, *83*, 111–136. [CrossRef]

74. Gradzielski, M.; Hoffmann, I. Polyelectrolyte-Surfactant Complexes (PESCs) Composed of Oppositely Charged Components. *Curr. Opin. Colloid Interface Sci.* **2018**, *35*, 124–141. [CrossRef]

75. Madinya, J.J.; Tjo, H.; Meng, X.; Ramírez Marrero, I.A.; Sing, C.E.; Perry, S.L. Surface Charge Density and Steric Repulsion in Polyelectrolyte–Surfactant Coacervation. *Macromolecules* **2023**, *56*, 3973–3988. [CrossRef]

76. Schulze-Zachau, F.; Braunschweig, B. Structure of Polystyrenesulfonate/Surfactant Mixtures at Air–Water Interfaces and Their Role as Building Blocks for Macroscopic Foam. *Langmuir* **2017**, *33*, 3499–3508. [CrossRef]

77. Czakaj, A.; Kannan, A.; Wiśniewska, A.; Grześ, G.; Krzan, M.; Warszyński, P.; Fuller, G.G. Viscoelastic Interfaces Comprising of Cellulose Nanocrystals and Lauroyl Ethyl Arginate for Enhanced Foam Stability. *Soft Matter* **2020**, *16*, 3981–3990. [CrossRef]

78. Zawala, J.; Kosior, D.; Malysa, K. Formation and Influence of the Dynamic Adsorption Layer on Kinetics of the Rising Bubble Collisions with Solution/Gas and Solution/Solid Interfaces. *Adv. Colloid Interface Sci.* **2015**, *222*, 765–778. [CrossRef]
79. Dukhin, S.S.; Kovalchuk, V.I.; Gochev, G.G.; Lotfi, M.; Krzan, M.; Malysa, K.; Miller, R. Dynamics of Rear Stagnant Cap Formation at the Surface of Spherical Bubbles Rising in Surfactant Solutions at Large Reynolds Numbers under Conditions of Small Marangoni Number and Slow Sorption Kinetics. *Adv. Colloid Interface Sci.* **2015**, *222*, 260–274. [CrossRef]
80. Kosior, D.; Zawala, J. Initial Degree of Detaching Bubble Adsorption Coverage and the Kinetics of Dynamic Adsorption Layer Formation. *Phys. Chem. Chem. Phys.* **2018**, *20*, 2403–2412. [CrossRef]